# SIMULATION OF ZERO NET ENERGY HOMES

Affouda-Léon Biaou Michel A. Bernier Yan Ferron
Département de génie mécanique
École Polytechnique de Montréal
Montréal, Québec
affouda-leon.biaou@polymtl.ca michel.bernier@polymtl.ca yan.ferron@polymtl.ca

## ABSTRACT

This article presents the models and methods used to simulate a Zero Net Energy Home (ZNEH). The ZNEH studied here is equipped with photovoltaic (PV) panels for on-site electrical production and a geothermal heat pump for space heating and cooling and domestic hot water pre-heating.

Simulations are performed using TRNSYS 15.3 with the IISiBat 3 interface. All major components are simulated using standard TRNSYS components except for the ground-source heat pump and geothermal heat exchanger which are modelled using components from the TESS library or from in-house models.

A R-2000 type home located in Montréal and equipped with 85.4 $m^2$ of PV panels and a 2.5 tons ground-source heat pump is simulated. Results indicate that with such an arrangement it is possible to achieve a ZNEH. The ground-source heat pump reduces the electrical energy for space heating and cooling requirements as well as for water heating by about half when compared to an all-electric house. With this scenario, 13550 kWh are required from the PV panels on an annual basis to achieve a ZNEH.

## INTRODUCTION

The non-renewable nature and greenhouse gas (GHG) emissions associated with conventional forms of energy has lead the way to the current trend towards "greener" engineering designs. The building sector is no exception. For example, in Canada, buildings are responsible for about 31% of all the energy consumed while GHG emissions are of the order of 134 Mt (Ayoub et al. 2001). Building engineers, helped by visionary building owners and government agencies, have risen to the challenge and buildings consume less energy than before. However, it is possible to do more and Zero Net Energy Homes (ZNEH) are a step closer towards sustainability.

Zero net energy homes (ZNEH) are energy-efficient grid-connected buildings with on-site electrical production from renewable energy sources. ZNEH supply electrical energy to the utility when there is a surplus and draws from the same grid in the case of on-site energy production shortage. The goal of a ZNEH is to have a balance, on an annual basis, between the surpluses and the shortages. The ZNEH concept is attractive to reduce the energy consumption in residential buildings and the emissions of greenhouse gases. Furthermore, when ZNEH use grid electricity produced from renewable sources, such as hydropower in the province of Québec, then ZNEH can be considered to be self-sufficient in terms of operational energy requirements. ZNEH are also very attractive in regions where electricity is produced from non-renewable sources. For example, in Canada, on average, each kW produced by renewable energy (PV, wind …) reduces $CO_2$ emissions by 1.58 tons per year when replacing coal ; 1.30 tons per year when replacing oil ; and 0.73 tons per year when replacing natural gas (Ayoub et al. 2001).

In order to limit the size (and cost) of on-site electrical production, the building part of a ZNEH need to be well designed. Furthermore, it has to be equipped with efficient electrical appliances, and heating/cooling systems. One particularity of the present study is that space heating/cooling as well as partial heating of domestic hot water is accomplished using a high efficiency (COP >3) ground-source heat pump.

ZNEH have been the subject of many investigations around the world. For example, the National Renewable Energy Laboratory (NREL) in the USA has a ZNEH program with the goal of building 120,000 such houses and schools by 2020 with an expected total energy reduction of $44.31\times10^6$GJ per year and consequently a decrease of GHG emissions of $0.7\times10^6$ metric tons of equivalent $CO_2$ per year (EERE, 2000).

The ZNEH concept has been discussed in several papers. Kadam (2001) reviewed the available technologies for zero net energy buildings and looked at the economical feasibility of the concept. Basing his analysis on a ZNEH prototype in Florida, Kadam indicated that the payback period is 63 years with the component costs of 1998. Reducing the price by half can reduce the payback period to 34 years.

Gilijamse (1995) studied the feasibility of using zero-energy houses in the Netherlands. The author used TRNSYS TYPE 56 to model the house and TUTSIM (a program for engineering design and optimisation which simulates dynamics systems) to simulate the heat demand with current best practices and advanced systems. Three configurations of zero-energy houses

all using PV electricity have been studied. Space heating and domestic hot water heating was provided either by using solar collectors in combination with seasonal storage or by additional photovoltaic cells feeding an electric heat pump. Gilijamse showed that zero-energy houses are feasible in the Netherlands and that cost-effectiveness can be achieved only for advanced systems with a heat pump configuration.

ZNEH are not limited to the use of photovoltaic panels for on-site electrical production. For instance, as suggested by Iqbal (2004) wind energy can be used. Using the HOMER software from NREL, Iqbal concluded that a 10 kW wind turbine could generate enough energy to satisfy the energy requirements of a R-2000 house in Newfoundland.

As mentioned in most studies, the main drawback of PV-driven ZNEH is the relatively long payback period. However, the rate at which the PV market increases and the current climate change challenge will contribute to make this technology attractive in the near future. Over the last 25 years, 1000 MW of PV power has been installed around the world with half that capacity installed in the last four years alone. The current rate of increase of PV production is around 26% per year and the cost-effectiveness of PV electricity is expected to be reached by 2020-2030 (Ayoub et al. 2001).

## PRINCIPLE OF OPERATION OF A ZNEH

A schematic representation of the ZNEH used in the present study is presented in Figure 1. The main components are: PV arrays for electricity generation; an inverter that transforms the direct current delivered by the PV array into alternative current required by the load; the local electric grid; a ground-source heat pump for space heating and cooling ; and a desuperheater (included in the heat pump) for domestic water pre-heating. Thermal or electrical energy is exchanged at several levels in this ZNEH. First, the PV generator (array+inverter) produces electricity that is fed to all appliances requiring electricity. The house is also connected to the electrical grid which can be considered to act as an energy storage device. When the PV system generates more energy than needed the surplus is sent to the grid. Conversely, when the PV output is insufficient to cover the house power demand, the grid supplies the required power. Usually, some form of net metering is used to measure the energy exchange in both directions (Messenger and Ventre, 2004). The objective of a ZNEH is to have an equal amount of electrical energy leaving and entering the house over a certain period (usually a year).

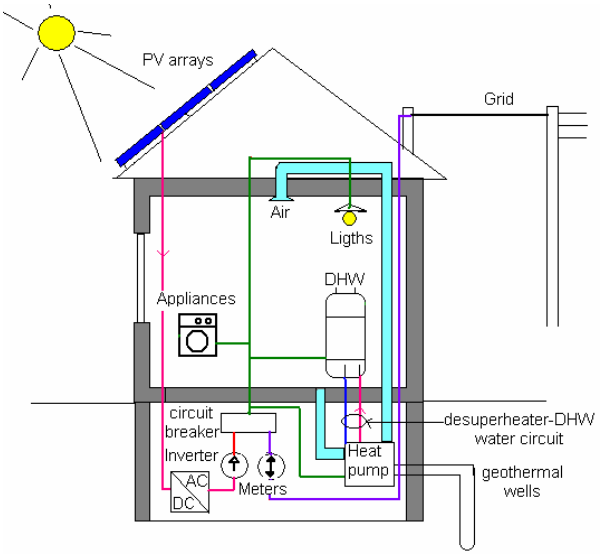


Figure 1: Schematic representation of the ZNEH studied.

The second set of energy exchange concerns the ground-source heat pump (GSHP) which has two liquid circuits and an air circuit. The first liquid circuit links the heat pump to the ground via a ground heat exchanger. With this set up, the ground is used as a heat source/sink for space heating or cooling and domestic hot water pre-heating. In heating, the heat pump captures heat from the ground to provide heat to the air circuit of the house and to pre-heat the domestic hot water. In cooling, the refrigeration cycle is reversed and the heat pump now removes heat from the house air circuit; part of the rejected heat is used to pre-heat the domestic hot water and the rest is rejected into the ground. The second liquid circuit is coupled to the desuperheater of the GSHP. A desuperheater is a heat exchanger that captures part of the energy contained in the hot refrigerant leaving the compressor and transfers it to a water circuit that preheats the domestic hot water. This preheated water is then pumped to a domestic hot water tank. Final water heating is accomplished inside the water tank using regular resistance heaters.

## SIMULATION

The ZNEH is simulated using the TRSNYS 15.3 simulation engine with the IISIBAT 3.0 interface (Klein, et al, 2000). Components models come from three sources: the TRNSYS standard models; models built in-house for this project; and models from the TESS library (TESS, 2001). The following paragraphs describe each component with an emphasis on the non-standard components.

**House.** The building simulated is a two-story 156 $m^2$ residential house with an unheated half-basement. The house characteristics are given in Table 1. The level of insulation is similar to that encountered in a R-2000 house which typically uses at least 30% less energy than a common house (ENERINFO Advisor, February 2000). The house is modelled using TRNSYS's TYPE 56 as three distinct thermal zones: living quarters,

attic, and basement. The last two zones are unconditioned and, therefore, the temperatures in these spaces are free-floating. TYPE 56 uses internally-generated conduction transfer functions to calculate transient heat conduction in the exterior walls and in the adjacent walls between the basement and the living space and between the attic and the living space. In this study, conduction transfer functions are generated based on a one hour time base.

The basement requires a special treatment since TYPE 56 can not model it directly. A new TYPE was therefore created, based on the work of Mitalas (1987), to calculate heat losses/gains from basement walls and floors (Dutil, 2003).

House infiltration is calculated using a technique presented by ASHRAE (1981). In this technique, the number of air changes per hour (ACH) is simply given by:

$$ACH = K1 + K2 \times (T_{zone} - T_{amb}) + K3 \times Windspeed \quad (1)$$

The values of K1, K2, K3 are respectively equal to 0.1, 0.011, and 0.034. These values are recommended by ASHRAE for a tightly sealed construction. Based on preliminary simulations it was found that the mean value of ACH ranged from about 0.5 to 0.2 for winter and summer conditions, respectively.

The weather processing model uses standard TRNSYS TYPE 9 in the WYEC2 format (ASHRAE, 1997). It is assumed that the house is occupied by a family of four persons who perform light work. This represents a heat gain of 150 W per person based on ISO7730. The four occupants are present from midnight to 8h and from 17h to 24h while only two are in the house from 8h to 17h. The hourly electrical power demand profile from the electrical appliances and the lighting is presented in Figure 2 (Gunes et al., 2003). As shown, the electrical load reaches a minimum of 0.15 kW at 2h and a maximum of 1.63 kW at 19h. It is assumed that the entire electrical load is instantly converted into heat and thus becomes a heat gain. The domestic hot water consumption profile used in the present study is given in Figure 3. It is based on a study by Perlman and Mills (1985).

**Ground source heat pump.** The GSHP model used in this study was first developed by TESS (TESS, 2001) as TYPE127. It has been modified by Lemire (1999) to account for the time of operation of the heat pump during a simulation time step. A thermostat TYPE, also written by Lemire (1999) controls the operation of the heat pump. It calculates the time of operation required, during a simulation time step, to maintain the heating and cooling set point temperatures. These set point temperatures are 20°C (with a deadband of 1°C) in heating and 25°C in cooling. In this study, the modeled

Table 1: House characteristics

| | |
|---|---|
| **Dimensions** | |
| Conditioned area | 156m$^2$ (6m×13m×2 floors) |
| Conditioned volume | 468m$^3$(6m×13m×3m×2 floors) |
| Roof area (south/north) | 88.4 m$^2$/64.35m$^2$ |
| Attic volume | 187.2m$^3$ |
| Basement (height/volume) | 1.5m/117m$^3$ |
| Window area | 14m$^2$ |
| East/south/west/north | 1.4/7/1.4/4.2 m$^2$ |
| **Envelop** | |
| Window | Double pane, low-e, Argon, insulated spacer<br>U=1.5 W/m$^2$°C,<br>SHGC=0.596 |
| Conditioned space wall<br>R=4.74 m$^2$°C/W | 102 mm Brick<br>12.7mm air layer<br>150 mm mineral wool<br>12.7 mm gypsum board |
| Conditioned space floor<br>R=3.77 m$^2$°C/W | 150 mm conc. (2400 kg/m$^3$)<br>125 mm mineral wool<br>19 mm gypsum board |
| Conditioned space ceiling<br>R=8.92 m$^2$°C/W | 310 mm mineral wool<br>12.7 mm gypsum plaster |
| Basement wall<br>R=3.57 m$^2$°C/W | 200 mm conc. (2400 kg/m$^3$)<br>115mm mineral wool |
| Roof<br>R=0.3 m$^2$°C/W | 6 mm shingles<br>12.7 mm plywood |
| | PV arrays on the south<br>Tilted at 45° |

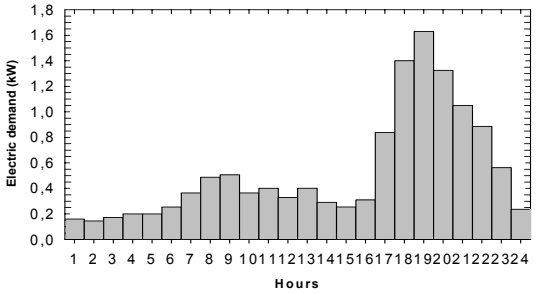


Figure 2: Lights and appliances electrical load profile.

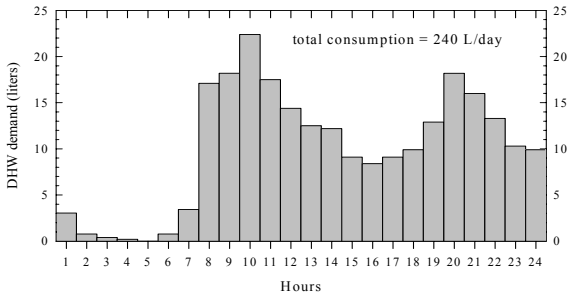


Figure 3: Hourly domestic hot water consumption.

heat pump is based on a commercially-available GSHP (ClimateMaster, 1995). It has a nominal cooling capacity of 2.5 tons (8.75 kW). It can operate with loop temperatures from 4.4°C to 43.3°C in cooling and from -3.5°C to 26.7°C in heating. Manufacturer's data were curve-fitted according to a procedure outlined by Lemire (1999). The resulting correlations and the corresponding data are shown on Figure 4 where it can be shown that the agreement between the correlations and the manufacturer's data is excellent.

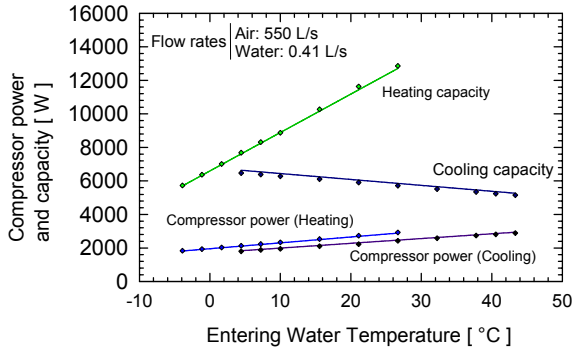


Figure 4: Heat pump performance data.

**Hot water heating**. As shown in Figure 5, domestic water heating is accomplished using a desuperheater coupled to a regular hot water tank equipped with electrical heating elements. The desuperheater is a refrigerant-to-water heat exchanger located between the compressor and the condenser. It is often found as an option on some GSHP models. As shown in Figure 5, a circulator pumps the cold water from the bottom of the tank to the desuperheater where the hot refrigerant gases heat the incoming water. Then, the heated water re-enters the hot water tank near the top. The desuperheater used in the present study operates only when the heat pump is providing space conditioning. In other words, the circulator is activated when there is a space conditioning need (heating or cooling). In cooling mode, the heat exchange in the desuperheater reduces the load on the condenser and, consequently, the amount of heat rejected to the ground.

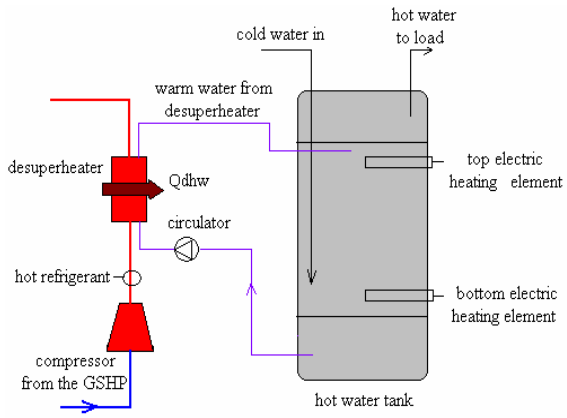


Figure 5: Domestic hot water pre-heating using a desuperheater.

This "free" energy would have been lost to the ground without a desuperheater. In heating, the heat recovered in the desuperheater translates into a loss of space heating capacity normally provided by the condenser of the GSHP. Thus, the heat pump would have to operate for a longer period to meet the space heating requirements. In this case, the hot water produced is not "free" but nonetheless obtained with a relatively high COP. The original TYPE 127 was modified to model the heat transfer from the desuperheater to the water. This heat transfer, denoted here by the expression $Q_{dhw}$, is given by:

$$Q_{dhw} = c_0 + c_1 T_{in,gshp} + c_2 T_{in,gshp}^2 + c_3 \dot{m}_w + c_4 \dot{m}_w^2 + c_5 T_{in,gshp} \dot{m}_w \quad \text{(in kW)} \quad (2)$$

where $T_{in,gshp}$ (in °C) and $\dot{m}_w$ (in $m^3/s$) are the fluid inlet temperature and flow rate on the GHE side of the GSHP, respectively. The coefficients $c_0$ to $c_5$ were obtained by curve-fitting manufacturer's data. These coefficients are given in Table 2.

Table 2 Coefficients used in Equation 2

| | Heating | Cooling |
|---|---|---|
| $c_0$ | 0.622553465 | 0.8084253 |
| $c_1$ | 0.0331952776 | 0.0532855 |
| $c_2$ | $-3.1182 \times 10^{-5}$ | $3.0760 \times 10^{-5}$ |
| $c_3$ | 960.891509 | - 29.20673 |
| $c_4$ | - 324411.498 | - 30694.289 |
| $c_5$ | 6.44317172 | - 31.893414 |

Typically, $Q_{dhw}$ is of the order of 1.5 kW which represents approximately 15% of the total GSHP capacity. It should be noted that the manufacturer does not provide any indication on the effect of the water temperature coming from the hot water tank. Therefore, it is assumed that $Q_{dhw}$ is independent of this temperature. It can be shown that the manufacturer's data and Equation 2 agree within ±2% and ±3% for cooling and heating mode, respectively.

The warm water produced by the desuperheater is fed to a regular 210 litres (1.5m high) electrical hot water tank. TYPE 60 of TRNSYS is used to model this tank. As shown in Figure 5, the tank has two inlets and two outlets. The cold water inlet is located 0.1 m from the bottom and the hot water outlet exists at the top of the tank. Water going to the desuperheater is taken 5 cm from the bottom of the tank (in order to have the coldest possible temperature at the inlet of the desuperheater) and returned to the tank at a height of 1 m (to avoid mixing the incoming warm water with hot water in the top portion of the tank). Two 0.75 kW resistance heaters provide the supplementary power to

heat the water to the set point temperature of 55 °C. These elements are located 0.3 and 1 m from the bottom of the tank, respectively. They operate in master/slave mode, with the highest priority assigned to the top element.

**Ground heat exchanger**. The closed-loop ground heat exchanger (GHE) used in this study consists of a U-tube made of high density Polyethylene (HDPE) inserted into a borehole. The GHE model used in this study is the one developed by the Department of Mathematical Physics from the University of Lund (Sweden) which has been implemented as a TRNSYS TYPE by Hellström et al. (1996). The main parameters used for the GHE are presented in Table 3. The borehole length of 100m was determined to be sufficient to avoid feeding the GSHP with fluid at a temperature below its minimum acceptable inlet temperature of -3.5°C.

Table 3: Main characteristics of the GHE

| Parameter | Value |
|---|---|
| Number of boreholes | 1 |
| Borehole length | 100 m |
| Undisturbed ground temperature | 10 °C |
| Ground thermal conductivity | 2.0 W/m-K |
| Storage heat capacity | 2000 kJ/m$^3$-K |
| Borehole diameter | 15 cm |
| U-tube | 1" SDR-11 |
| U-tube center-to-center distance | 8.3 cm |
| Grout thermal conductivity | 2.08 W/m-K |
| Pipe thermal conductivity | 0.42 W/m-K |

**Photovoltaic system.** On-site electrical production is accomplished using a photovoltaic (PV) array composed of a series of PV modules which themselves are composed of PV cells. PV cells are semiconductor devices that convert sunlight into direct current (DC) electricity (Messenger and Ventre, 2004). Single crystal silicon cells are used in the present study. They supply the house with electrical energy with the surplus being fed to the grid; no on-site electrical storage is provided.

The PV array is modelled using TRNSYS's TYPE 94. TYPE 94 uses a so-called "four parameter" model which treats a PV as an irradiance and temperature dependent current source connected in parallel with a diode and in series with a resistor and the load (Fry, 1998). This model is briefly described below.

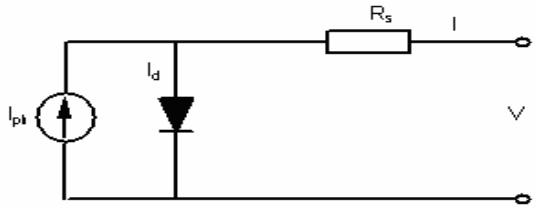


Figure 6: Equivalent circuit of a four-parameter PV model.

The equivalent circuit is shown in Figure 6 where $I$ and $V$ represent the load current and voltage, respectively. The useful power is given by the product of these two electric characteristics.

The diode current, $I_d$ , is given by (Fry, 1998):

$$I_d = I_s \left[ \exp\left( \frac{q}{\gamma k T_c} (V + IR_s) \right) - 1 \right] \qquad (3)$$

where $I_s$ is the reverse saturation current, $\gamma$ is a dimensionless diode curve-fitting factor with a minimum possible value equal to the number of cells in series in the module $N_s$, $k$ is the Boltzmann constant (1.38066 × $10^{-23}$ J/K), $q$ is the electron charge (1eV or 1.60218×$10^{-19}$ C), $R_s$ is the module series resistance (Ω), $T_c$ is the cell temperature (K), and $V$ is the voltage across the PV module (Volts).

The photocurrent, $I_{ph}$, is proportional to the solar radiation reaching the PV cell. The current generated by the module, $I$, is simply the difference between the photocurrent and the diode current:

$$I = I_{ph} - I_d \qquad (4)$$

The four parameters of the model are: $I_{ph}$, $I_s$, $R_s$, and $\gamma$. The reverse saturation current depends on the semiconductor material characteristic and the cell temperature (Carlin and al. 1996):

$$I_s = BT_c^3 \exp\left( -\frac{E_b}{AkT_c} \right) \qquad (5)$$

$A$ is a constant (= $\gamma/N_s$ ), $E_b$ is the semiconductor band gap energy at 0 K ( 1.12 to 1.79 eV for silicon cells) and B is a material constant estimated using manufacturer's data. The model considers $R_s$ and $\gamma$ to be constants while $I_{ph}$ and $I_s$ depend on the operating conditions: $I_s$ varies with cell temperature and $I_{ph}$ depends on the incident irradiance. The 1.22 m$^2$ PV modules used in this study are made of 72 solar cells connected in series with a peak power of 140 W and a conversion efficiency of 11.5% at so-called "Standard Test Conditions". They are produced for grid-connected systems by a leading manufacturer of solar cells. The PV module characteristics are summarized in Table 4 and in Figure 7.

As can be seen, manufacturer's data do not provide directly the four parameters needed to run TYPE 94. These parameters are evaluated internally by TYPE 94 using a methodology described by Eckstein (1990). The underlined values in Table 4 are required by TYPE 94 to calculate these four parameters.

As shown in Figure 7, the electrical output of the PV cell is influenced by its operating temperature, $T_{cell}$. It is possible to account for this temperature dependence by using temperature coefficients applied to the short circuit current, $I_{sc}$, the open circuit voltage, $V_{oc}$, and the maximum power $P_{mpp}$ (Patel, 1999):

$$I_{sc} = I_{sc,ref} \times (1 + \alpha_{Isc} \times [T_{cell} - T_{cell,ref}]) \quad (6)$$
$$V_{oc} = V_{oc,ref} \times (1 - \alpha_{Voc} \times [T_{cell} - T_{cell,ref}]) \quad (7)$$
$$P_{mpp} = P_{mpp,ref} \times (1 - \alpha_{Pmpp} \times [T_{cell} - T_{cell,ref}]) \quad (8)$$

where $T_{cell,ref}$ , $I_{sc,ref}$ , $V_{oc,ref}$ , $P_{mpp,ref}$ are the cell temperature, the short circuit current, open circuit voltage , and maximum power at the STC, respectively. The temperature coefficients are usually provided by manufacturers. In the present case, the values are given in the last column of Table 4. Using Equation 8 and the PV module used in this study, one can see that a 1°C rise in the cell temperature above the reference temperature decreases the maximum power by 0.45%. Thus, PV cells work better in cold climates.

Table 4: Characteristics of the PV module used in the present study.

| Standard Tests Conditions<br>1000W/m²; AM1.5;<br>cell temperature 25°C | | Nominal Operating Cell Temperature (NOCT) conditions<br>800W/m² ; AM1.5;<br>wind speed =1m/s;<br>Ambient temp. = 20°C | | Temperature coefficients | |
|---|---|---|---|---|---|
| Rated power | 140 W | Cell Temp. | 45°C | $\alpha_{Pmpp}$ | -0.45%/°C |
| Peak power current | 4.24 A | Mpp* power | 102 W | | |
| Peak power voltage | 33 V | Mpp voltage | 30.2 V | $\alpha_{Isc}$ | +2 mA/°C |
| Open circuit voltage | 42.8 V | Open circuit voltage | 39.2 V | $\alpha_{Voc}$ | -152 mV/°C |
| Short circuit current | 4.7 A | Short circuit | 3.8 A | *Mpp: maximum power point | |

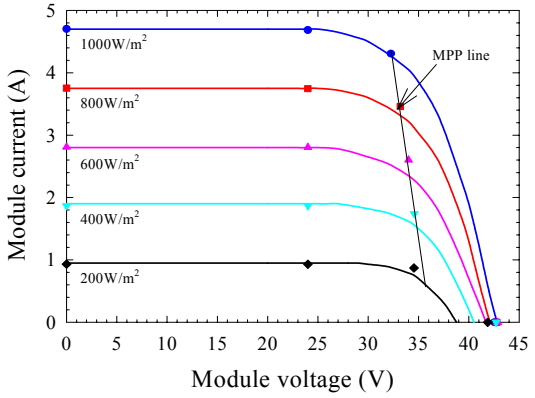


Figure 7: I-V curves for a cell temperature of 25°C and different irradiance levels. Manufacturer's data (curves) and results from TYPE 94 (data points).

The four-parameter TYPE 94 PV model has been validated several times (Fry, 1998). As a further check and to verify its implementation in the present study, its outputs were checked against manufacturer's data.

Some results of this verification are presented in Figure 7 where four sets of data points are shown for each irradiance level. They represent (from left to right): the short circuit current, the array current, the maximum power point (MPP) and the open circuit voltage, respectively. In each case, the agreement between the outputs of TYPE94 and the manufacturer's data is very good.

It is important to note that, depending on the load characteristics, the cell can operate anywhere on a given I-V curve and not necessarily at the MPP. Fortunately, PV arrays are usually coupled to inverters which, in addition to converting direct current to alternative current, "seek" the optimal power point of the PV arrays by using a maximum power point tracker. The TYPE 94 model assumes that the PV array is connected to such an inverter. Therefore, during a simulation, TYPE 94 uses the manufacturer's data and the weather data to calculate the model parameters and provides, at each time step, the maximum power point.

TRNSYS as an inverter model as one of its standard component (TYPE 48). It is a relatively simple model which assumes that the DC/AC conversion is accomplished at constant (user-specified) conversion efficiency. A conversion efficiency of 95% is used in the present study based on data taken from commercially available devices. In essence, TYPE 48 gets as inputs the array power and the house load power requirements and outputs the excess power output from the array.

## RESULTS

Results presented in this section are based on the house described in Table 1. Figure 8 shows the hourly space conditioning loads of this house for the Montréal climate. As shown, the peak heating and cooling loads are approximately 9.0 and 3.3 kW, respectively. Annually, space heating and cooling energy requirements are 13905 and 1742 kWh, respectively.

The annual energy needs for domestic water heating are 4986 kWh while lights and appliances require 4659 kWh. Overall, if one assumes that the house is electrically heated (space and water) and cooled with an electrically-driven air-conditioning with a COP of 3, then the amount of electricity needed by the house is 24131 kWh (and 14485 kWh for space heating and cooling requirements).

Figures 9 and 10 present various electrical power demands for the same house equipped with 85.4 $m^2$ of PV panels and a GSHP for space conditioning and domestic water pre-heating. Figure 9 presents data for a typical winter week while Figure 10 is for a typical summer week. The first three curves in each figure present the average hourly power requirements of the

DHW tank, the GSHP, and the lights and appliances while the fourth one gives the total of the first three.

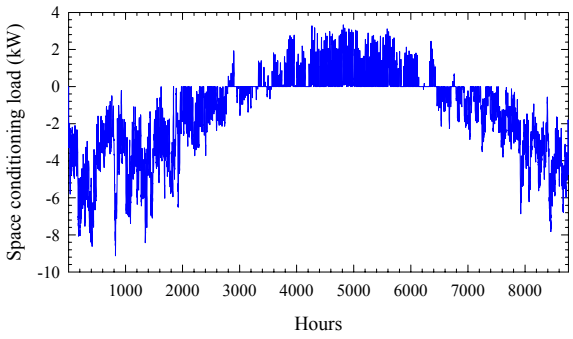


Figure 8: Hourly space heating and cooling loads.

It can be seen that the power required in the DHW tank peaks at 0.75 kW (maximum power of the heating element in the tank) while the power required by lights and appliances peak at the hourly average value of 1.63 kW in accordance with Figure 2. During the weeks shown in Figures 9 and 10, the maximum average hourly power demand required by the GSHP is 2.0 and 1.15 kW, respectively. The resulting maximum power requirements for the winter and summer weeks are 3.85 and 2.9 kW, respectively.

The top three curves in Figures 9 and 10 give the PV module output, the total power demand and the power deficit (= total power demand – PV output). As can be seen, the peak power produced by the PV arrays is greater in the winter week (≈ 9.9 kW) than in the summer week (≈ 7.7 kW). This is fairly representative of the winter/summer difference in PV output. In fact, the maximum PV output occurs near the spring equinox (≈ 11.4 kW) and the minimum near the summer solstice (≈ 8 kW) based on an examination of the yearly values (not presented here). This difference is due to two factors. First, the cell temperatures are lower in winter than in summer. As indicated earlier, there is performance improvement of the order of 0.45% per $^{o}$C below 25$^{o}$C. Secondly, the sun angle striking the PV array (inclined at 45$^{o}$) is more favourable at the equinox than at the solstice.

The peak power produced by the PV panels is lower in summer. However, the insolation duration is longer in summer as can be noticed by comparing the width of the PV peaks in Figures 9 and 10. Therefore, the energy produced per day is higher in the summer months. As can be seen in Figures 9 and 10, the deficit is negative during the daytime hours for both the winter and summer weeks indicating a surplus of electrical energy production by the PV panels.

On an annual basis, the GSHP consumes 5735 kWh for space conditioning and water pre-heating (which represents only 39.5% of the raw space heating and cooling requirements). Domestic hot water heating requirements drop to 2472.5 kWh (from 4986 kWh) due to water preheating by the GSHP desuperheater.

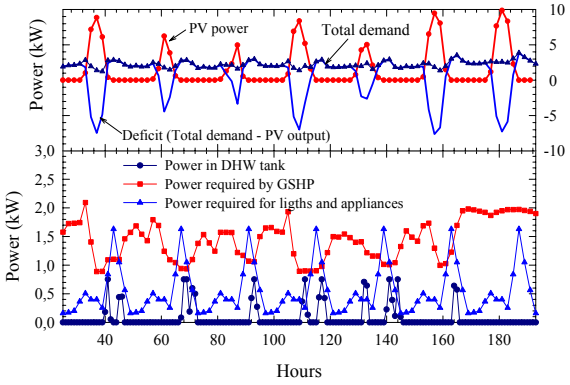


Figure 9: Power requirements and production for a typical winter week.

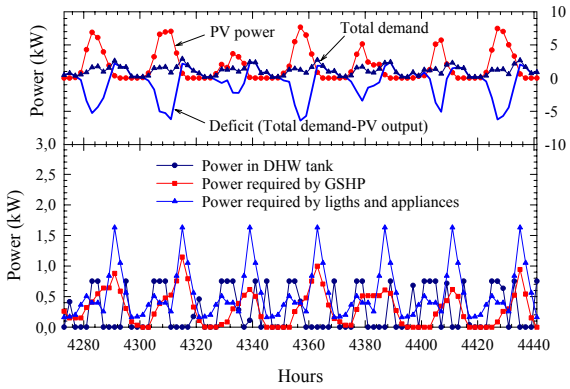


Figure 10: Power requirements and production for a typical summer week.

Figure 11 shows the annual cumulative energy balance of the ZNEH. The total annual electrical consumption is 13550 kWh. As indicated in Figure 11, as the year progresses the deficit shifts from a positive to a negative value with the inflection point located around mid-year. The PV production is 13655 kWh and the annual energy balance is almost zero (105 kWh) indicating that a ZNEH is possible.

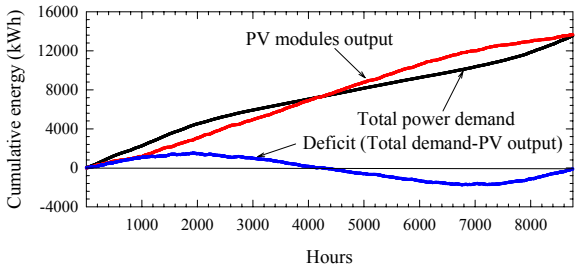


Figure 11: Cumulative energy requirements and production.

## CONCLUSION

This article presents the models and methods used to simulate a Zero Net Energy Home (ZNEH). The grid-connected ZNEH studied here is equipped with photovoltaic (PV) panels for on-site electrical production and a ground-source heat pump for space heating and cooling and domestic water pre-heating. Simulations are performed, using TRNSYS 15.3 with the IISiBat 3 interface, on a R-2000, 156m$^2$ home located in Montréal.

Overall, if one assumes that the house is electrically heated (space and water) and cooled with an electrically-driven air-conditioning with a COP of 3, then the amount of electricity needed by the house is 24131 kWh. When this house is equipped with a 2.5 tons ground-source heat pump, the annual amount of electricity required drops to 13550 kWh. It is shown that this level of electricity production can be accomplished using 85.4 m$^2$ of south-facing PV panels titled at 45°. On an annual basis, the grid supplies more electricity than it receives from the PV panels in the winter. However, the situation is reversed in the summer and overall, there is a near zero net energy balance at the end of the year.

## REFERENCES


ASHRAE (1981). Handbook of fundamentals, Chapter 26.

ASHRAE (1997). WYEC2, Weather Year for Energy Calculations. ASHRAE, Inc. Atlanta.

Ayoub, J., Dignard, L., Filion, A. (2001). Photovoltaics for buildings: opportunities for Canada.. CANMET-CTEC Number 2001-123(TR)/21-12-2001.(http://cetc-varennes.nrcan.gc.ca/eng/publication/r2001-123f.html).

ClimateMaster (1995). E Series – E030 model, Water source heat pumps.

Dutil, Jean-Pier (2003). Création d'un programme sur TRNSYS permettant de calculer les pertes de chaleur dans un sous-sol, Projet de fin d'études, département de génie mécanique, École Polytechnique de Montréal.

Eckstein, J.H. (1990). Detailed Modelling of Photovoltaic System Components, M.Sc. thesis, University of Wisconsin – Madison.

EERE (2000). Zero Net Energy Buildings, Outreach and action Plan. (http://www.eere.energy.gov/solarbuildings/pdfs/ zne.pdf).

ENERINFO Advisor (2000). Building an Energy Efficient Home. Nova Scotia Department of Natural Resources.

Fry, B. (1998). Simulation of Grid-Tied Building Integrated Photovoltaic Systems. M.Sc. thesis. University of Wisconsin - Madison.

Gilijamse, W. (1995). Zero-energy Houses in the Netherlands. In: Proceedings of IBPSA 95. Madison, Wisconsin, USA, August 14-16, 1995. 276-283.

Gunes, B. M., Ellis, M.W. (2003). Evaluation of Energy Environmental, and Economic Characteristics of Fuel Cell Combined Heat and Power Systems for Residential applications. ASME Trans.. Vol. 125. 208-220.

Hellström, G., Mazzarella, L., Pahud,D. (1996). Duct ground storage model – TRNSYS version. Department of Mathematical Physics, University Of Lund, Sweden.

Iqbal, M.T. (2004). A Feasibility Study of a Zero Home in Newfoundland. Ren. Energy 29. 277-289.

Kadam, S. (2001). Zero net Energy Buildings: Are they economically feasible? Sustainable Energy Proceedings. http://web.mit.edu/10.391j/www/proceedings/Kadam2001.pdf

Klein, S.A., et al. (2000). "TRNSYS - Reference Manual". Solar Energy Laboratory, University of Wisconsin-Madison. Madison, WI (USA).

Lemire, N. (1999). Étude sur les systèmes de pompes à chaleur géothermiques, M.Sc.A., département de génie mécanique, École Polytechnique de Montréal.

Messenger, R.A., Ventre, J. (2004). Photovoltaic Systems Engineering, 2nd edition, CRC press.

Mitalas, G.P. (1987). Calculation of below-grade residential heat loss: low-rise residential buildings, ASHRAE Transactions, Vol. 93, part 1.

Patel, M. R, (1999). Wind and Solar Power Systems. CRC press.

Perlman, M., Mills, B.E. (1985). Development of Residential Hot Water Use Patterns, ASHRAE Transactions, vol. 91, part2, pp.657-679.

TESS (2001). http://www.tess-inc.com